Journal of Optoelectronics and Advanced Materials Vol. 7, No. 5, October 2005, p. 2727 - 2735

ULTRASOUND ROLE IN SOL-GEL PROCESSING OF $PbTiO_3$ CERAMICS

I. Chilibon[*], J. Marat-Mendes[a], R. Igreja[a], C. J. Dias[a]

National Institute of Research and Development for Optoelectronics, INOE-2000, 077125,
PO Box MG-5, Bucharest, Romania
[a]Department of Materials Science, Faculty of Science and Technology, New University of
Lisbon, 2829-516 Caparica, Portugal

Lead titanate ($PbTiO_3$) powders in tetragonal form have been successfully prepared by sol-gel method. The processing of lead titanate ceramics was followed up using techniques such as: X-ray diffraction (XRD), thermal analysis (DSC) and microscopy (SEM). Three lead titanate powders have been obtained in different conditions function of annealing temperature and ultrasound field. The sol-gel process may be improved by ultrasound gel irradiation in an optimum irradiation time, and implies the structure homogeneity of PT powders. The ceramic powder, which had ultrasound irradiated gel, exhibited higher Curie temperature than ceramic powders obtained in the typical sol-gel process.

(Received May 25, 2005; accepted September 22, 2005)

Keywords: Sol-gel, Lead titanate, $PbTiO_3$, PT, Ultrasound

1. Introduction

Lead titanate ceramic type $PbTiO_3$, (PT), which exhibits a perovskite structure and high Curie temperature of 490 ^oC belong to the most important ferroelectric and piezoelectric families [1]. PT ceramics have many important ferroelectric and piezoelectric technological applications in optoelectronics and microelectronics, because of their high Curie temperature, pyroelectric coefficient and spontaneous polarisation. Ferroelectric ceramics, as lead titanate show a high electromechanical coupling coefficient, k_t, a large range of dielectric constant values and low dielectric and mechanical losses. However, these ceramics have high acoustic impedance and low flexibility [2].

New chemistry routes utilized to process lead titanate ceramics are: sol-gel, hydrothermal reactions, co-precipitation, and emulsion technique. We used the sol-gel method, due to its advantages, specifically: the reactants are mixed on a molecular level, a better control of stoichiometry, higher purity raw materials, the easy formation of ultra-fine and crystallized powders [3]. Also, the preparation of the ceramic powders by sol-gel technique allows one to obtain pure ceramic powders with controlled morphology and grain size [4].

In the sol-gel process the precursors for preparation colloid consists of a metal or metalloid element surrounded by various ligands. Metal alkoxides are popular precursors because they react readily with water. The reaction is called hydrolysis, because a hydroxyl ion becomes attached to the metal atom. Two partially hydrolysed molecules can link together in a condensation reaction. Condensation liberates a small molecule, such as water. A gel is a substance that contains a continuous solid skeleton enclosing a continuous liquid phase. The continuity of the solid structure gives elasticity to the gel. Gelation can be produce by rapid evaporation of solvent, as occurs during preparation of films or fibres. Gelation can occur after a sol is cast into a mould, in which case it is possible to make objects of desired shape. Aging of gel may involve further condensation, dissolution

---

[*] Corresponding author: qilib@yahoo.com

and reprecipitation of monomers, or phase transformation within the solid or liquid phases. Drying by evaporation under normal conditions gives rise to capillary, pressure that causes shrinkage of gel network. Most gels are amorphous, even after drying, but many crystallize when heated. Once a gel has been densified, it is equivalent to a ceramic made by conventional. After gel has been melted, however, it "forgets" its manner of preparation and acquires the equilibrium structure dictated by thermodynamics [5].

Power ultrasound can be used to improve the crystallization process, but this requires an appreciation of all the phenomena occurring during sonocrystallization. Applying ultrasound to crystallizing systems offers a significant potential for modifying and improving both the processes and the products. Ultrasound waves might have influence on the growth rate and the crystals size distribution during crystallization in saturated solutions [6], however the nucleation rate of the crystals can be increased several times with ultrasound. The crystal growth rate depends on the ultrasonic frequency and intensity, and several authors have noted this acceleration of the crystals growth under ultrasound for different solutes, however today the mechanism of the ultrasound action is not yet well understood [6]. A possible explanation is that the ultrasonic wave increases the probability of collision between the particles as in the primary nucleation. Therefore, we can say that the effects of ultrasound on crystallization process are very divers, mostly positive, but that they are numerous and difficult to analyse separately.

2. Experimental procedure

Preparation of the ceramic powders type $PbTiO_3$ by sol-gel method utilised in our investigation involves several steps, such as: preparation of solutions, gelation, gel drying, and thermal processes for conversion into amorphous powders and crystallisation.

The method of preparation of lead titanate (PT) and characterization of these gels has been described in a previous publication [7].

$PbTiO_3$ ceramics were prepared utilising as precursors Titanium (IV) isopropoxide $Ti[OCH(CH_3)_2]_4$, 99.99% purity and Lead(II) acetate trihydrate $Pb(CH_3COO)_2{\cdot}3H_2O$, 99% purity, and 2-methoxyethanol $CH_3OCH_2CH_2OH$ as solvent. Preparation of $PbTiO_3$ gel was realized according to Schwartz studies [8], with some modifications, such as the reaction time, and hydrolyses conditions. Also, by utilizing nitrogen atmosphere flux the distillation process was faster.

The gel was prepared by addition of equal volumes of precursor solution (sol) and a solution, containing water (Rw = 2.5) and 2-methoxyethanol as solvent. So, the gelation of solutions was controlled through a hydrolytic polycondensation, by water adding. In the drying process, the densification and removal of volatile compounds, induce some modifications into the gel structure, solvent removal leads to microporosity and therefore the area surface increases. During the gel conversion into amorphous powder through a thermal process, hidroxy groups and some organic residuals are exothermic removed and induce appropriate mass decrease. Thereby, the water removal and burning of residual compounds, network collapses while the structure relaxes, and viscous sintering continues until the porous phase is eliminated. Densification of the amorphous gels by thermal process implies structure relaxation, polymer condensation and viscous sintering. In the preliminary drying gel process (Fig. 1), the gel put into a silicon oil bath, is heated at 200 ^{0}C for 12 hours into a glass bottle, and continuously mixed by a spinner. After that, the amorphous powder was heated into an oven at 300 ^{o}C for 24 hours. Secondarily, the drying process was made into an oven at 500 ^{o}C for 2 hours, and we obtained an amorphous powder. After that, the amorphous powder was crystallised into an oven at 800 ^{o}C for 2 hours (Fig. 2), through out from oven and cooled in air.

In our work we obtained three kinds of $PbTiO_3$ samples, namely A, D2b, and C (ultrasound irradiated gel). By utilizing the first route for sol-gel process we realized powder sample, namely type A. In the modified sol-gel route, the gel was heated at 550 ^{o}C for three hours, and then at 800 ^{o}C for two hours. In this case we obtained the D2b sample.

In order to study the effects in the structure and morphology powders, at ultrasound irradiation, we modified the first process route. Therefore, before the drying process we made an ultrasound irradiation to the gel, during 40 minutes. First of all, the glass bottle with gel was immersed into an ultrasound bath, heated at 40 °C. A piezoceramic sandwich transducer generated into water ultrasound vibrations at 35 kHz resonant frequency. Ultrasonic vibrations were propagated through the gel and induced cavitation effects. After ultrasound gel irradiation we made the preliminary drying of gel at 200 °C, but only for one hour, instead of 12 hours, that means a much shorter time like for A sample, in order to obtain C sample. One objective was to decrease the entire process duration, without damaging the final properties of the ceramic powder.

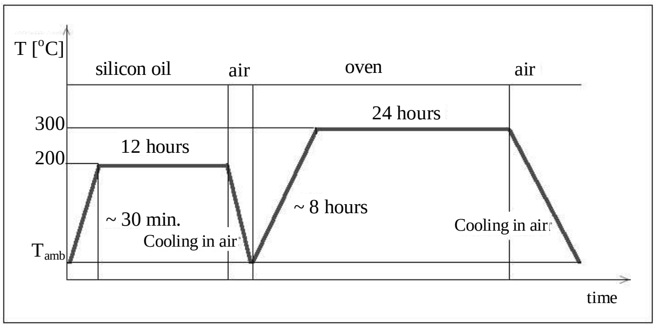

Fig. 1. Preliminary drying gel process.

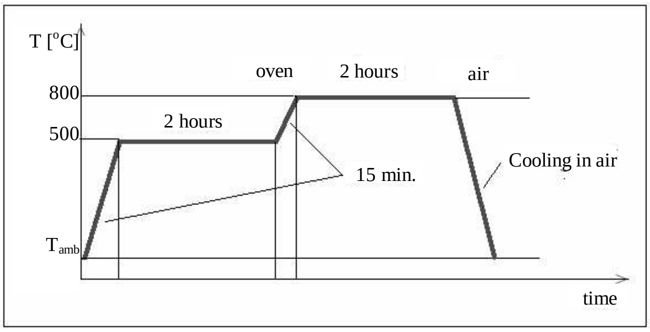

Fig. 2. Drying process of amorphous powder.

3. Ceramic powders characterisation

SEM, XRD and DSC analysis investigated the crystallisation and morphology properties of ceramic powders. The Rigaku DMAX-III C diffractometer has a Copper and Cu K-alpha radiation on the diffracted beam, with 1.5405 nm wavelength. The c/a ratio for the powders was calculated from X Ray Diffraction. The ceramic powders type A and D2b present tetragonal mode, with c = 4.1532 nm and **a** = 3.8993 nm, that means **c/a** = 1.0651. The ceramic powder type C presents tetragonal mode, with **c** = 4.9871 nm and **a** = 3.9675 nm, that means **c/a** = 1.257.

The XRD diffractograms for the ceramic powders A, D2b and C, treated at 800 °C for 2 hours, are presented in Fig. 3. It points out for all powders, as the presence of peaks corresponds to the perovskite phase. In the case of C powder, there is a small 2θ shift that indicates c/a ratio growth of crystalline network.

The thermal characteristics of ceramic powders were obtained by utilising the DSC 92 Differential Scanning Calorimeter, SETARAM, France in 400 °C to 500 °C temperature range, and 5 °C/min temperature rate. Figs. 4, 5, and 6 present the curves of heat flow function of temperature for A, D2b and C samples.

In the case of C powder, the Curie temperature, indicated by the endothermic peak is 485.69 ^{0}C that is 0.41 °C greater than to the A sample. Further, by decreasing temperature in DSC process, we obtained the exothermic temperature peak of C sample at 485.22 °C that is 7.06 °C greater than to the A sample.

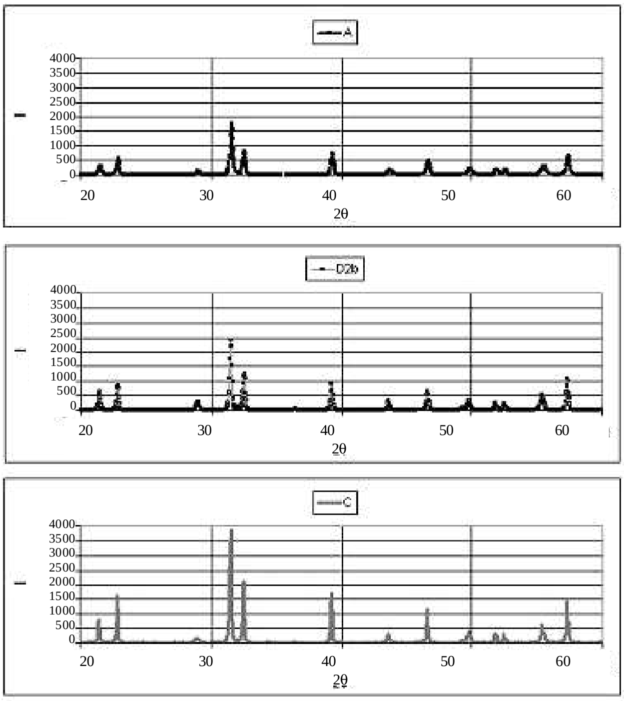

Fig. 3. X Ray Diffraction of PT ceramic powders (A, D2b, and C samples), heat-treated at 800 ^{o}C for two hours.

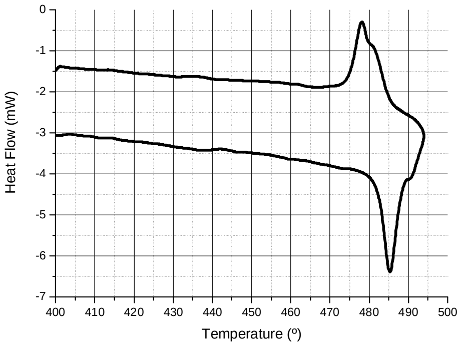

Fig. 4. Heat flow curve function of temperature for A sample.

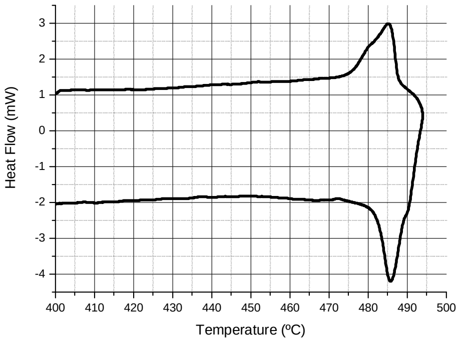

Fig. 5. Heat flow curve function of temperature for C sample.

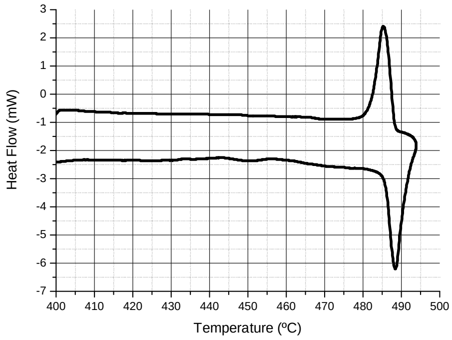

Fig. 6. Heat flow curve function of temperature for D2b sample.

D2b sample presents T_{endo} = 488.487 ºC endothermic temperature peak with - 6.19667 mW heat flow, and T_{exo} = 485.331 ºC exothermic temperature peak with 2.407671 mW heat flow (Fig. 6).

Values of heat flow peaks represent the endothermic and exothermic temperatures, and are presented in the Table 1, for the A, D2b and C samples, where: T_{endo} and T_{exo} are endothermic and exothermic temperatures, Hf_{endo} and Hf_{exo} are endothermic and exothermic heat flows in T_{endo} and T_{exo}.

The ΔH enthalpies for endothermic and exothermic peaks have been calculated by the relationship:

$$\Delta H = \text{Heat flow area}/[\text{mass x (temperature rate)}]$$

where: “mass” is the sample mass utilized in DSC experiments (28.6 mg) and the “temperature rate” is 5 ^{0}C/s.

Endothermic peaks of the heat energy for A and C samples are presented in Figs. 7 and 8. Also, the Figs. 9 and 10 show the exothermic peaks of the heat energy for A and C samples. Correspondently to the previously relationship, the values of calculated enthalpies are presented in the Table 2.

Table 1. Thermal characteristics of A, D2b and C samples.

Characteristic	A sample	D2b sample	C sample
T_{endo} [^{0}C]	485.28	488.48	485.69
Hf_{endo} [mW]	- 6.3845	- 6.197	- 4.2013
T_{exo} [^{0}C]	478.16	485.33	485.22
Hf_{exo} [mW]	- 0.2966	2.4077	2.9856

Table 2. Enthalpies for PT samples.

PT sample	Endothermic area [mJ]	Exothermic area [mJ]	ΔH_{endo} [J/g]	ΔH_{exo} [J/g]
A	115.00	137.74	0.804	0.963
C	92.87	143.43	0.649	1.003

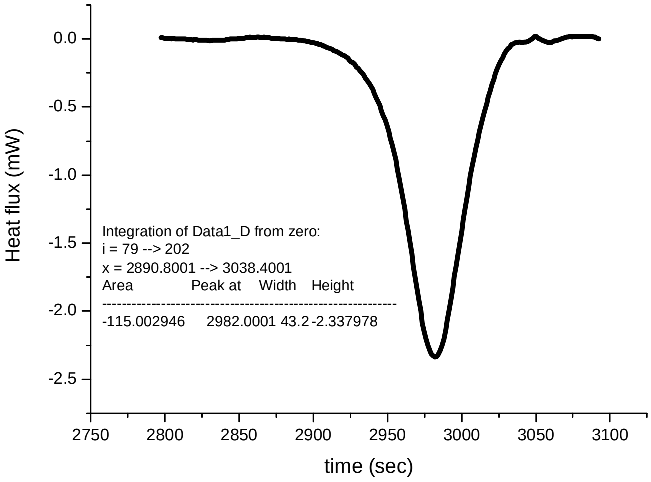

```
Integration of Data1_D from zero:
i = 79 --> 202
x = 2890.8001 --> 3038.4001
Area            Peak at    Width    Height
--------------------------------------------------------------
-115.002946     2982.0001 43.2 -2.337978
```

Fig. 7. Thermal energy in endothermic peak for A sample.

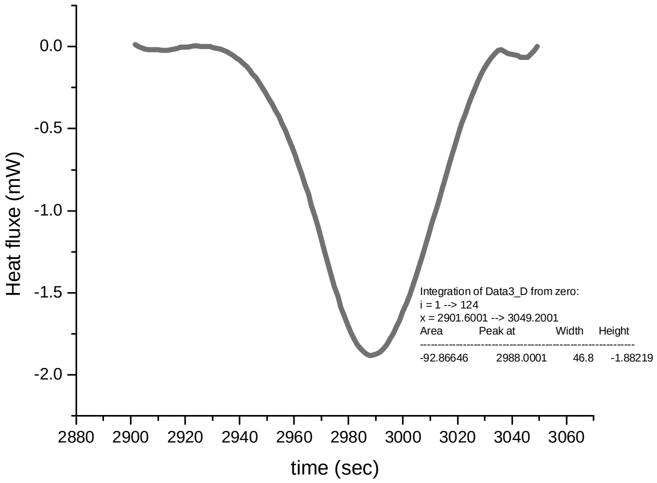

```
Integration of Data3_D from zero:
i = 1 --> 124
x = 2901.6001 --> 3049.2001
Area          Peak at          Width    Height
------------------------------------------------------------
-92.86646       2988.0001       46.8    -1.88219
```

Fig. 8. Thermal energy in endothermic peak for C sample.

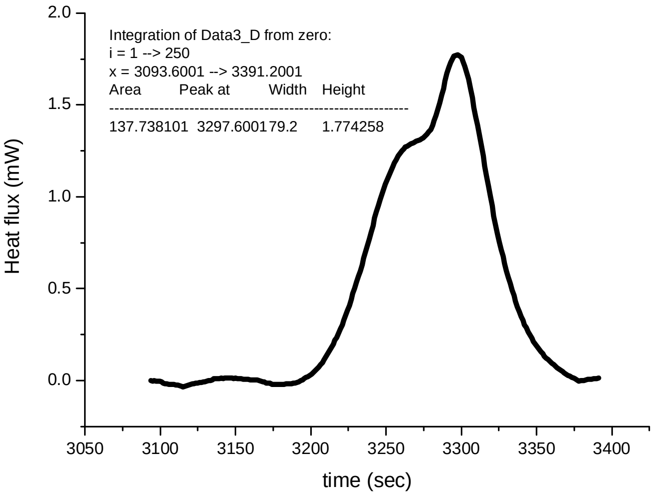

```
Integration of Data3_D from zero:
i = 1 --> 250
x = 3093.6001 --> 3391.2001
Area        Peak at        Width    Height
-------------------------------------------------------------
137.738101  3297.600179.2       1.774258
```

Fig. 9. Thermal energy in exothermic peak for A sample.

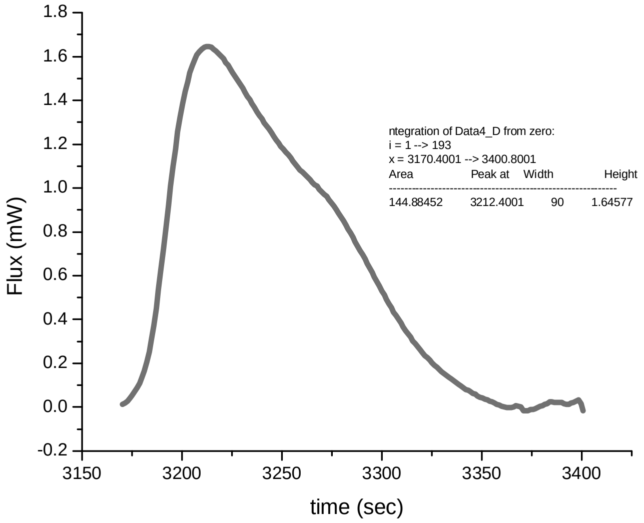

```
ntegration of Data4_D from zero:
i = 1 --> 193
x = 3170.4001 --> 3400.8001
Area            Peak at   Width           Height
------------------------------------------------------------
144.88452       3212.4001      90      1.64577
```

Fig. 10. Thermal energy in exothermic peak for C sample.

Utilizing the Digital Scanning Microscope, type ZIESS – DSM962, Germany, it has revealed the morphology and grain sizes of PT powders. The SAM micrographs presented in Figure 11 show grater size grains for C sample, comparatively with the grains of A and D2b sample. Also, D2b sample presents very well formed grains.

As an application of PT ceramics, we prepared 0-3 connectivity composite material utilizing the method described in [9], [10], vicelike A ceramic powder and P(VDF-TrFE) powder at 50% volume loading of ceramic. Both powders (PT and P(VDF-TrFE)) were mixed together into agate mortar and suited amount of acetone was poured over the mixture. The solid mass formed was then hot pressed, in order to obtain composite film of 100 μm thicknesses. Aluminium electrodes were deposited on both sides of the composite film by vacuum evaporation. The composite film was polarised into a silicon oil bath with an applied electric field (DC field) of 20 MV/m at 109 ^{o}C for 30 minutes. Fig. 12 shows the hysteresis loop for PT: P(VDF-TrFE) measured at 0.1 Hz, where the switching polarisation was computed only with the switching current measured on the sample.

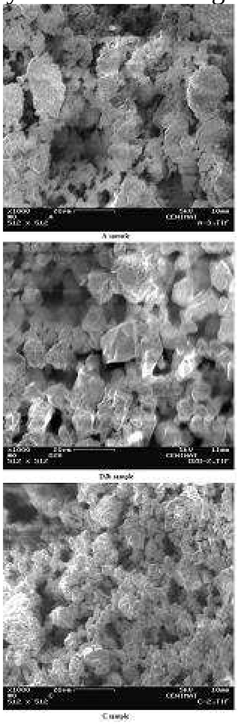
A sample

D2b sample

C sample

Fig. 11. SEM micrographs of PT powders (A, D2b, and C samples).

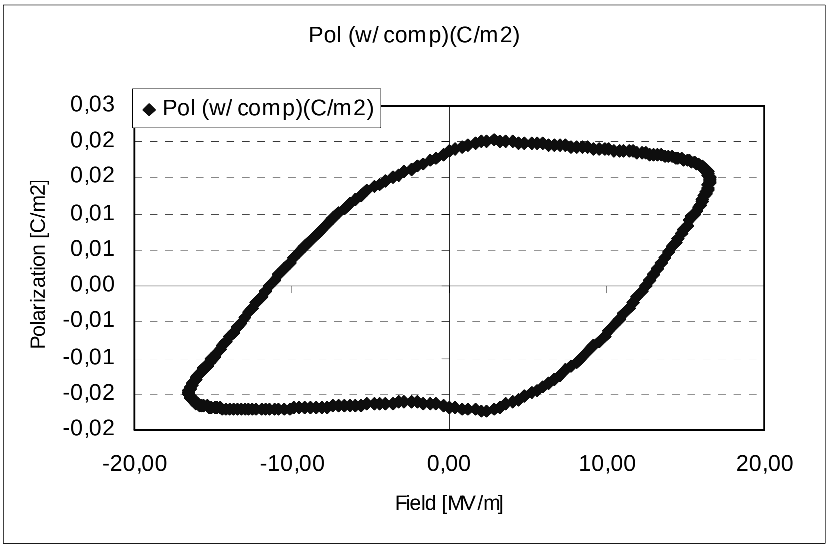

Fig. 12. Ferroelectric hysteresis loop for PT: P(VDF-TrFE) composite film.

4. Discussions

The sol-gel method allowed obtaining pure ceramic powders with controlled morphology and small grain size. Thermal analysis made between 400 ºC to 500 ºC temperature range, revealed as every one of three powders yielded thermal hysteresis.

Three sol-gel routes were used to create PT powders. Ultrasound utilization in the sol-gel process of PT crystalline powders was proposed, in order to obtain crystal grains in a shorter time process [11]. Crystallization preparation by a thermal process of crystalline ceramics depends on the process duration. Also, the temperature conditions have great influence in the growth of crystal size.

All crystallised ceramic powders (A, D2b, and C samples) presented thermal hysteresis, and high ferroelectric-paraelectric transition temperatures. The Curie temperature, indicated by the endothermic peak for C sample is 485.69 °C that is 0.41ºC greater than to the A sample.

D2b sample presents T_{endo} = 488.487 ºC endothermic temperature peak with - 6.197 mW heat flow, and T_{exo} = 485.33ºC exothermic temperature peak with 2.4077 mW heat flow.

In DSC process, by decreasing temperature, we obtained the exothermic temperature peak of C sample at 485.22 °C that is 7.06 ºC greater than to the A sample. Also, endothermic and exothermic peaks of temperature show higher values for the C ultrasound sample, comparatively with those to the A ceramic sample obtained in the classic process sol-gel. However, the ultrasound powder has smaller temperature hysteresis.

It has been observed that the crystalline structure of PT powder type C has been modified by ultrasound irradiation. This phenomenon might be explained by favourable forming of crystalline grains at ultrasound field application. It points out that all PT ceramic powders exhibit peaks appropriate to the perovskite phase. However, in the case of C powder, there is a small 2θ shift that indicates an increase of c/a ratio of crystalline network. Thereby, XRD analysis has shown grater c/a ratio and good crystallization for the ultrasound sample.

Crystalline structure for C powder was obtained in shorter time by ultrasound gel irradiation, pursuant to a better crystal formation. Ultrasound irradiation implies a better nucleation, and has a benefit influence on the growth rate and the distribution of crystals.

In the second sol-gel process route we obtained D2b sample, which presents very well formed grains. So, the heating of gel about 3 hours at 550 °C temperature, that means one hour longer time than for the other two routes, may contribute to better crystallization of grains and better homogeneity.

The morphology of PT powders, analysed by ZIESS – DSM962 Digital Scanning Microscope, Germany, and revealed in SAM micrographs, shows a grater size for the grains in A sample, comparatively with C sample.

5. Conclusions

Ultrasound irradiation implies a better nucleation. It has been observed that ultrasonic waves have an influence on the size-growing rate of crystals and the crystals size distribution.

The sol-gel technique allows obtain pure ceramic powders with controlled morphology and grain size. As consequence, it is possible to enhance these material properties. Further studies are in progress to see the influence of different morphologies and grain sizes of these powders on electric, dielectric, ferroelectric, piezoelectric and pyrolectric properties of the ceramic-polymer composite thin films.

In conclusion, the sol-gel process may be improved by ultrasound gel irradiation, controlling the irradiation time and implies the structure homogeneity of PT powders.

References

[1] J. Fang, J. Wang, S. C. Ng, C. H. Chew, L. M. Gan, J. Mater. Science **34**, 1943 (1999).
[2] C. Dias, PhD Thesis, University of Wales, Bangor, 1994.
[3] S. Kazaoui, J. Ravez, J. Mater. Sci. **28**, 1211 (1993).
[4] R. Igreja, C. J. Dias, J. N. Marat-Mendes, Ferroelectrics **228**, 99 (1999).
[5] C. J. Brinker, G. W. Scherer, SOL-GEL SCIENCE. The Physics and Chemistry of Sol-Gel Processing, Academic Press, New York, 1990.
[6] N. Amara, B. Ratsimba, A. Wilhelm, H. Delmas, Ultrasonics Sonochemistry **11**, 17-21 (2004).
[7] R. Igreja, C. J. Dias, J. N. Marat-Mendes, J. Sol-Gel Science and Technology **8**(1-3), 721 (1997).
[8] R. W. Schwartz, University of Illinois at Urbana-Champain, USA, Thesis, 1989.
[9] R. Igreja, C. J. Dias, J. N. Marat-Mendes, 10th Intern. Symposium on Electrets, 631 (1999).
[10] C. J. Dias, R. M. Marat-Mendes, P. Inacio, J. N. Marat-Mendes, D. K. Duas Gupta, IEEE Transactions on Dielectric and Electrical Insulation **11**(1), 35 (2004).
[11] J. Marat-Mendes, I. Chilibon, R. Igreja, M. Carmo, C. Dias, P. Inácio, Proc. European Micro and Nano Systems 2004, EMN04, Advances&Applications for Micro & Nano Systems, ESIEE, Noisy le Grand – Paris, France, 149 (2004).